Ultrasonic study of the charge-fluctuation compound Sm_3Te_4

Yuichi Nemoto and Terutaka Goto
Graduate School of Science and Technology, Niigata University, Niigata 950-2181, Japan

Akira Ochiai
Material Science and Technology, Niigata University, Niigata 950-2181, Japan

Takashi Suzuki
The Institute for Solid State Physics, The University of Tokyo, Tokyo 106-8666, Japan
(Received 23 July 1999)

We have measured the ultrasonic velocity and attenuation coefficient of the rare-earth chalcogenide Sm_3Te_4 to examine the valence-fluctuation effect due to the coexistence of Sm^{2+} and Sm^{3+} ions in the ratio of 1:2. The ultrasonic dispersion around 120 K indicates that the charge-fluctuation time obeys the activation-type temperature dependence $\tau=\tau_0\exp(E/k_BT)$ with a characteristic time $2\pi\tau_0=2.5\times10^{-13}$ sec and an activation energy $E=0.136$ eV. The absence of the phase transition due to the charge ordering in Sm_3Te_4 means a freezing of Sm^{2+} and Sm^{3+} ions in random distribution at low temperatures. We find an elastic softening with $\ln T$ dependence below 15 K down to a spin glass transition around 1.3 K. This striking behavior is attributed to a two-level system due to the tunneling of $4f$ electrons among randomly distributed Sm^{2+} and Sm^{3+} ions. This result is similar to the ionic tunneling in amorphous glass compounds. Employing the group-theoretical analysis, we show some aspects of charge-fluctuation modes in Sm_3Te_4 and a possible mechanism for the charge glass state of Sm^{2+} and Sm^{3+} ions.

I. INTRODUCTION

Most of the rare-earth elements in their chemical composites favor trivalent states. The compounds including Sm, Eu, Tm, and Yb elements very often show the valence-fluctuation phenomena associated with the coexistence of their trivalent and divalent states.[1] The samarium chalcogenides Sm_3X_4 ($X=$S, Se, Te) with the Th_3P_4-type structure characterized by a cubic space group T_d^6 are well known as typical examples of a valence-fluctuation compound, where two different valence ions of Sm^{2+} and Sm^{3+} coexist.[2] The divalent Sm^{2+} ion has a $4f^6$ electronic configuration with ground-state multiplet $^7F_0$ and excited $^7F_1$ at about 400 K, while Sm^{3+} has a $4f^5$ configuration with ground-state multiplet $^6H_{5/2}$. It is expected that the charge neutrality is filled for the chemical composite consisting of two different valences as $Sm^{2+}(Sm^{3+})_2(X^{2-})_4$. Actually the magnetic susceptibility of Sm_3X_4 is explained by a sum of the susceptibility of the Van Vleck term for Sm^{2+} with $J=0$ (0 K) and $J=1$ (400 K), and of the Curie term for Sm^{3+} with $J=\frac{5}{2}$ in the coexistence ratio of $N(Sm^{2+}):N(Sm^{3+})=1:2$.[3,4]

A conventional unit cell of Sm_3X_4 ($X=$S, Se, Te) in Fig. 1 includes four molecular formulas. Both ions of Sm^{2+} and Sm^{3+} in Sm_3X_4 occupy crystallographically equivalent sites with S_4 symmetry and exhibit valence fluctuation due to the thermal hopping motion of $4f$ electrons among different valence states. The group of Sm_3X_4, therefore, is called an *inhomogeneously mixed valence* system.[1] We refer to Yb_4As_3 and Fe_3O_4 as similar mixed valence compounds, which show the charge ordering in lowering temperature. In the case of Yb_4As_3, the structural phase transition from a cubic to a trigonal phase is accompanied by the charge ordering of Yb^{3+} ions along the [111] direction below $T_c=292$ K.[5] The present compounds of Sm_3X_4, however, do not show the charge ordering even down to low temperatures.

The dc electric resistivity of Sm_3X_4 exhibits the thermal activation-type temperature dependence of $\rho=\rho_0\exp(E/k_BT)$.[3,6] The activation energy determined by the

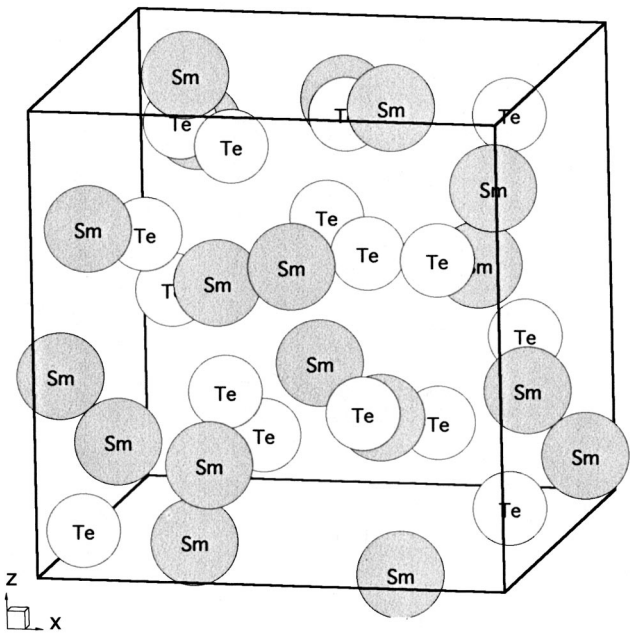

FIG. 1. Conventional unit cell of Sm_3Te_4 with the Th_3P_4-type structure belonging to the space group T_d^6. Four molecular formulas are included in the conventional unit cell.

dc resistivity shows a common value of $E=0.12-0.15$ eV for the three compounds Sm_3X_4 ($X=S, Se, Te$). The high-frequency dielectric response up to 1 GHz for Sm_3Se_4 measured by the admittance meter indicates that the dielectric dispersion of the Cole-Cole type is ruled by the thermal activation-type relaxation time of $\tau(E)=\tau_0 \exp(E/k_BT)$ with $E=0.14$ eV and $2\pi\tau_0=2.4\times10^{-13}$ sec.[7] Furthermore, the high-frequency resistivity of Sm_3Se_4 shows the carrier at low temperatures to be completely absent. Because Sm_3X_4 shows a common transport property, it is expected that the present compound Sm_3Te_4 is also characterized to be an insulator without a carrier at low temperatures.

The ultrasonic measurements of the elastic constant and attenuation coefficient for Sm_3Se_4 show a considerable dispersion around 120 K due to the thermal hopping motion of $4f$ electrons among Sm^{2+} and Sm^{3+} ions.[8] The relaxation time determined by the ultrasonic method obeys the activation-type temperature dependence $\tau=\tau_0 \exp(E/k_BT)$, which is consistent with the result observed by the high-frequency dielectric response.[7]

The low-temperature specific heat of Sm_3X_4 exhibits broad rounded peaks at 0.8 K (Sm_3S_4), 1.2 K (Sm_3Se_4), and 1.5 K (Sm_3Te_4) due to the spin glass transition.[9–11] The specific-heat anomaly shows a broad peak around a slightly higher temperature than the spin glass transition point T_g. The ac magnetic susceptibility of Sm_3Te_4 also shows a cusp around the spin glass transition of $T_g=1.3$ K. A pronounced irreversibility of low-temperature magnetization in zero field cooling and field cooling in Sm_3Te_4 is consistent with a metastable state of the spin glass phase.[12]

In the present paper, we show the ultrasonic measurements of Sm_3Te_4 and the dispersion effect due to the valence-fluctuation state. The low-temperature behavior of elastic constants is shown in connection with the two-level system of the $4f$ electrons in the random potential. An analysis for the charge-fluctuation modes and a possible mechanism for a formation of the charge glass state in Sm_3Te_4 are presented.

II. EXPERIMENT

A single crystal of Sm_3Te_4 was grown with a temperature gradient method in a W crucible sealed by electron-beam welding. The sample with a rectangular shape of $2.5\times2\times2$ mm^3 was prepared for the present ultrasonic measurement. The surfaces were polished with alumina powder to be plane parallel. The piezoelectric transducers of $LiNbO_3$ were bonded on the parallel surfaces of the sample for generating and receiving the ultrasonic wave. We employed the pulse-echo method for measurements of the ultrasonic velocity v by a homemade apparatus with the phase difference detector. The elastic constant $C=\rho v^2$ was derived from the mass density $\rho=7.450$ g/cm^3 with a lattice constant $a=9.5004$ Å of the present sample Sm_3Te_4. We used the MATEC system with an exponential-decay comparator for ultrasonic attenuation measurements. A homemade ^{3}He-evaporation refrigerator was used for the low-temperature measurements down to 0.4 K. The magnetic field up to 120 kOe was generated by a superconducting magnet.

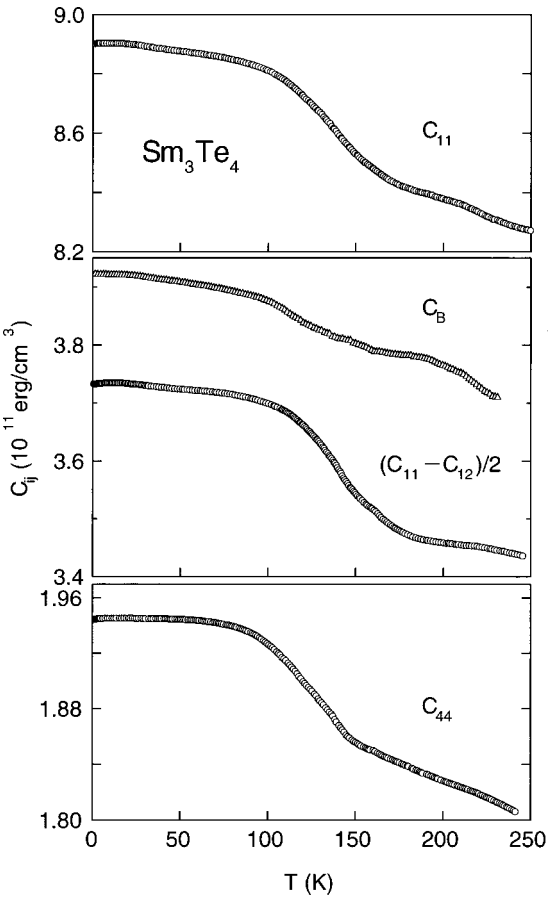

FIG. 2. Temperature dependence of the elastic constants C_{ij} of Sm_3Te_4. We measured the ultrasonic waves with frequencies 44 MHz for C_{11} and 48 MHz for $(C_{11}-C_{12})/2$, C_{44}. The bulk modulus C_B was calculated by the results of the longitudinal C_{11} and transverse $(C_{11}-C_{12})/2$ modes. The anomalies of C_{11}, $(C_{11}-C_{12})/2$, and C_{44} modes around 120 K are attributed to the ultrasonic dispersion.

III. RESULT AND DISCUSSION

A. Ultrasonic dispersion

Figure 2 shows the temperature dependence of the elastic constants C_{ij} of Sm_3Te_4. We used the longitudinal sound wave with a frequency of 44 MHz for the measurement of C_{11} and a transverse wave of 48 MHz for $(C_{11}-C_{12})/2$, C_{44}. The bulk modulus C_B in Fig. 2 is calculated from the experimental results of C_{11} and $(C_{11}-C_{12})/2$. It is noted that the anomalies of the elastic constants of Sm_3Te_4 in Fig. 2 resemble very well those of Sm_3Se_4.[8] This anomaly around 120 K is attributed to a dispersion effect, where the characteristic time $1/f=2\pi/\omega$ of the sound wave coincides with the relaxation time $2\pi\tau$ of the valence fluctuation in Sm_3Te_4. Therefore, the measurement of the attenuation coefficient for the ultrasonic waves with different frequency is important to determine the valence fluctuation time.

Open circles and squares in Fig. 3 show the temperature dependence of the attenuation coefficient α_{11} of Sm_3Te_4 for the longitudinal C_{11} mode with a fundamental frequency 14 MHz and its overtone 44 MHz, respectively The maximum position of α_{11} shifts to a high-temperature side with increasing frequency of the ultrasonic wave. We also present the elastic constant C_{11} with 44 MHz. In the analysis of the

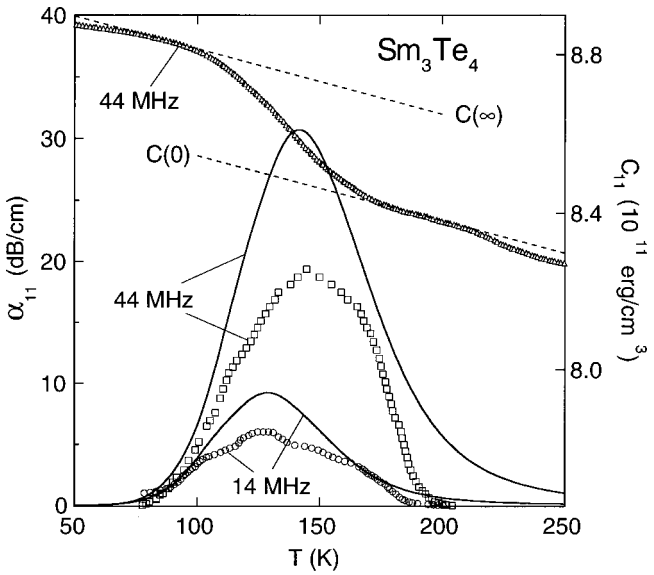

FIG. 3. Attenuation coefficient α_{11} of the longitudinal C_{11} mode with the sound wave frequencies 14 and 44 MHz. Temperature dependence of the elastic constant C_{11} is also shown. Solid lines are fits of α_{11} with Eq. (1) based on the Debye-type dispersion. $C(\infty)$ denotes a high-frequency limit and $C(0)$ a low-frequency limit.

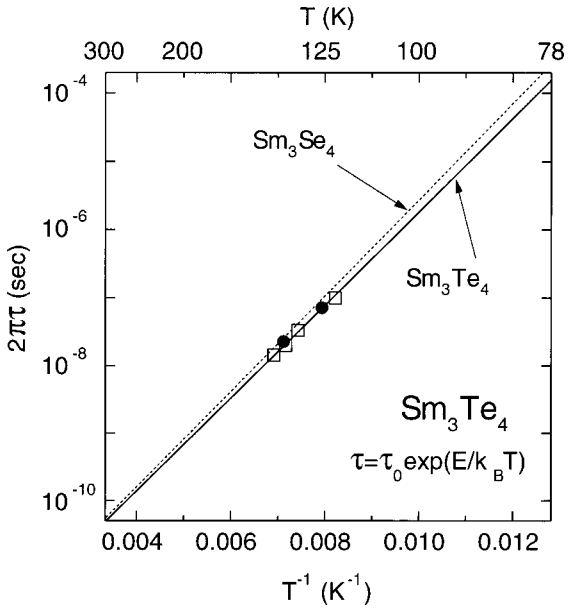

FIG. 4. The relaxation time $2\pi\tau$ determined by the ultrasonic attenuation in Sm_3Te_4. The previous result of Sm_3Se_4 is also presented for comparison. Solid circles are results of Sm_3Te_4 and open squares are of Sm_3Se_4. The solid and dashed lines mean the activation-type temperature dependence $\tau=\tau_0\exp(E/k_BT)$ with the parameters in the text.

ultrasonic attenuation of Fig. 3, we assume the Debye-type dispersion with single relaxation time $\tau(E)$. For the ultrasonic wave with angular frequency $\omega=2\pi f$, the attenuation coefficient α_ω is written as

$$\alpha_\omega=\frac{\Delta C}{2\rho v^3}\int dE\,\frac{G(E)\omega^2\tau(E)}{1+\omega^2\tau(E)^2}. \tag{1}$$

$\Delta C=C(\infty)-C(0)$ is the difference of the elastic constants for a high-frequency limit $C(\infty)$ and a low-frequency limit $C(0)$. In order to describe the distribution of the relaxation time $\tau(E)$ of the charge fluctuation, we introduce a Gaussian distribution function $G(E)$ for an activation energy as

$$G(E)=\frac{1}{\sqrt{2\pi}D}\exp\left[-\frac{1}{2}\left(\frac{E-E_0}{D}\right)^2\right]. \tag{2}$$

Here E_0 is the center of the distribution of the activation energy. The solid lines in Fig. 3 based on Eqs. (1) and (2) with $E_0=0.136$ eV and $D=0.020$ eV reproduce the experimental result of the attenuation α_{11}. We use $C(\infty)=(8.98-0.001\,65T)\times10^{11}$ erg/cm^3 and $C(0)=(8.71-0.001\,65T)\times10^{11}$ erg/cm^3 for high- and low-frequency limits, respectively.

The solid line in Fig. 4 shows the relaxation time $2\pi\tau$ of Sm_3Te_4 with the activation-type temperature dependence $\tau=\tau_0\exp(E/k_BT)$. The experimental result of $2\pi\tau$ in Sm_3Se_4 is also presented in Fig. 4 for comparison. We obtained a characteristic time for a high-temperature limit $2\pi\tau_0=2.5\times10^{-13}$ sec and an activation energy of $E_0=0.136$ eV in Sm_3Te_4, which are almost equal to the previous results of $2\pi\tau_0=2.4\times10^{-13}$ sec and $E_0=0.14$ eV in Sm_3Se_4.[7,8] The present experiment indicates that the elastic properties of Sm_3X_4 (X=S, Se, Te) also resemble each other.

In a low-temperature limit, the valence fluctuation rate of Sm_3Te_4 becomes infinite without long-range ordering and both Sm^{2+} and Sm^{3+} ions are frozen to be spatially random distribution. This behavior is in contrast to the usual second-order phase transition, where the critical slowing down of the fluctuation time gives rise to the long-range ordering. In the present system of Sm_3Te_4, it is expected that a kind of frustration effect prevents the long-range charge ordering due to the Coulomb interaction. Even though the crystalline electric-field state of the $4f^5$ of Sm^{3+} and the $4f^6$ of Sm^{2+} ions in the potential with tetragonal S_4 symmetry has been observed by the neutron scattering,[13] the intersite interaction for the magnetic moments is strongly affected by the random distribution of Sm^{3+} and Sm^{2+} ions in the system. Actually the spin glass phase is observed in Sm_3Te_4 below $T_g=1.3$ K.[12] In the next section, we present the elastic anomalies around the spin glass transition.

B. Low-temperature anomaly

In Fig. 5 we show the low-temperature behavior of the elastic constants C_{ij} of Sm_3Te_4 in expanded scales. The longitudinal C_{11} mode and the transverse $(C_{11}-C_{12})/2$,C_{44} modes exhibit noticeable softening about 0.02–0.04 % below 15 K and show upturns around the spin glass transition $T_g=1.3$ K. It should be noted that the low-temperature softening has been observed in $(C_{11}-C_{12})/2$ and C_{44} modes associated with symmetry-breaking shear strains, while the bulk modulus C_B of the volume strain with total symmetry shows a monotonous increase in lowering temperature.

The softening of the longitudinal C_{11} mode in Fig. 6 shows a logarithmic temperature dependence of $\ln T$ below 11 K and shows a minimum around the spin glass transition of $T_g=1.3$ K in zero field. Even in magnetic fields parallel to the [100] direction the softening of $\ln T$ has also been observed. As shown in the inset of Fig. 6, the minimum point

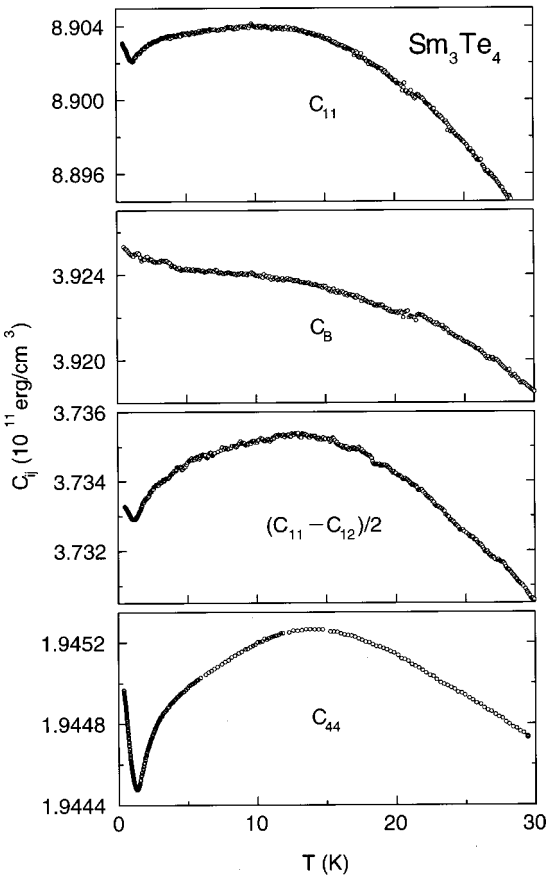

FIG. 5. Low-temperature behavior of the elastic constants of C_{ij} in Sm_3Te_4. The C_{11}, $(C_{11}-C_{12})/2$, and C_{44} modes exhibit softening below 15 K and show upturns around the spin glass transition $T_g=1.3$ K.

of the spin glass transition gradually shifts to a low-temperature side with increasing magnetic field.

It has been found that the glass compounds show characteristic low-temperature properties of the specific heat $C=\gamma T$, the thermal conductivity $\kappa=AT^2$, and the elastic softening with $\ln T$ dependence. These properties are attributed to the two-level system, which is caused by the tunneling motion of ions in the random potential of the glass compounds.[14–17] As shown in the preceding section, the charge glass state is formed by the random distribution of Sm^{2+} and Sm^{3+} ions in Sm_3Te_4. Therefore, we propose that the two-level system due to the tunneling motion of the $4f$ electron in the random potential gives rise to the low-temperature softening with $\ln T$ dependence in Fig. 5. In the analogy of ionic tunneling in glass compounds, we write a low-temperature softening of elastic constant $\Delta C/C$ as[16,18]

$$\frac{\Delta C}{C}=\frac{2\Delta v}{v}=\frac{2[v(T)-v(T_0)]}{v(T_0)}=\frac{2\bar{P}\gamma^2}{\rho v^2}\ln\left(\frac{T}{T_0}\right)$$
$$=2K\ln\left(\frac{T}{T_0}\right). \quad (3)$$

Here, v is the velocity of ultrasound, $\bar{P}$ is the density of the two-level system, γ is the coupling constant of the ultrasonic wave with the two-level system, and T_0 is the reference temperature. The $\ln T$ dependence of the elastic constants of

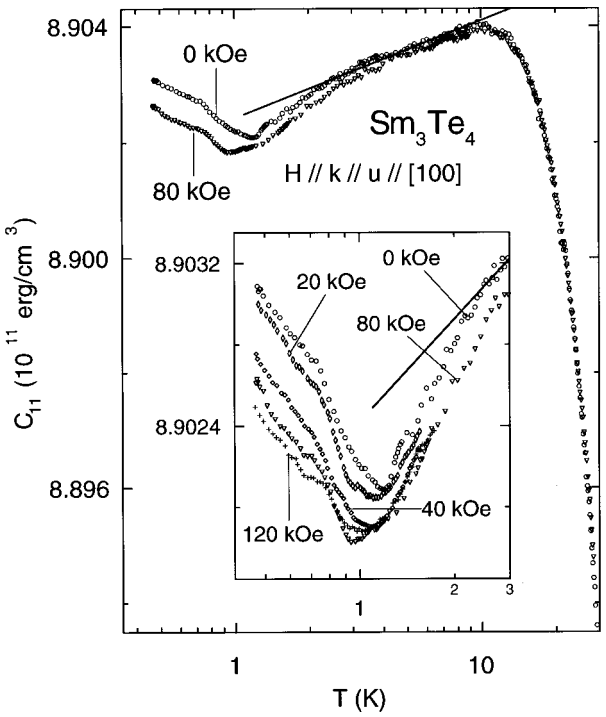

FIG. 6. Elastic constant of C_{11} of Sm_3Te_4 under magnetic fields parallel to the propagation direction [100] of the longitudinal ultrasonic wave. Solid line is a fit to determine tunneling parameters from Eq. (3) in the text with $T_0=11$ K and $K=0.44\times10^{-4}$.

amorphous glass compounds is caused by the tunneling of ions through random potentials.[19,20] The dimensionless parameter K in amorphous glass compounds is known to be a universal value of about 10^{-4}, which does not show the sample dependence.[20–22]

The thermal hopping motion of the $4f$ electrons across the potential barrier of $E=0.136$ eV in Sm_3Te_4 dies out completely at low temperatures. The tunneling motion of the $4f$ electrons among the randomly distributed Sm^{2+} and Sm^{3+} ions in Sm_3Te_4 plays an important role at low temperatures. In this context we propose that the $\ln T$ dependence of the elastic constant in Sm_3Te_4 is attributed to the two-level system of the $4f$ electron among randomly distributed Sm^{2+} and Sm^{3+} ions. The solid line of the C_{11} mode in Fig. 6 is obtained by Eq. (3) with the constant $K=\bar{P}\gamma^2/\rho v^2=0.44\times10^{-4}$.

The transverse $(C_{11}-C_{12})/2$ mode in Fig. 7 also shows a softening proportional to $\ln T$ below 12 K down to 1.3 K under zero field. In the case of $(C_{11}-C_{12})/2$, the minimum point at 1.3 K under zero field shifts to a low-temperature side under the magnetic field parallel to the [110]. We have deduced $K=1.4\times10^{-4}$ from the inclination of the solid line in Fig. 7.

The transverse C_{44} mode under magnetic fields in Fig. 8 also shows the logarithmic temperature dependence of $\ln T$ below 14 K. From the inclination of the solid line for C_{44} with Eq. (3) in Fig. 8, $K=0.71\times10^{-4}$ was derived. C_{44} becomes softer in decreasing the temperature towards the spin glass transition point around 1.3 K. The minimum point corresponding to the spin glass transition shifts to a low-temperature side with increasing magnetic field. This behavior is consistent with the results of C_{11} in Fig. 6 and $(C_{11}-C_{12})/2$ in Fig. 7.

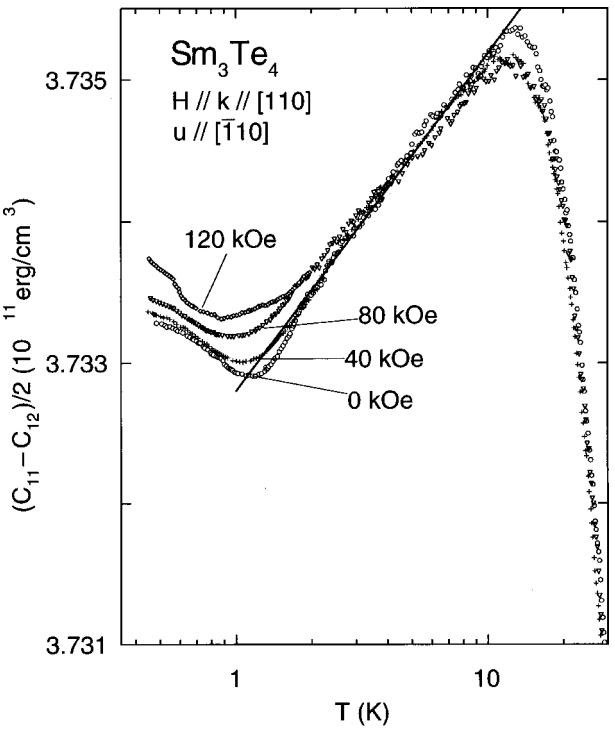

FIG. 7. Elastic constant of $(C_{11}-C_{12})/2$ of Sm_3Te_4 under magnetic fields parallel to the propagation direction [110] of the transverse ultrasonic wave. Solid line is a fit from Eq. (3) in the text with $T_0=13\,\mathrm{K}$ and $K=1.4\times10^{-4}$.

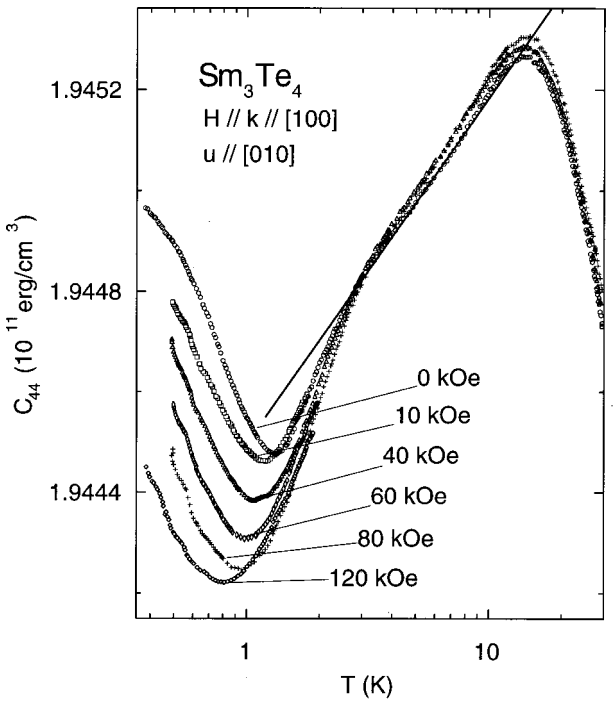

FIG. 8. Elastic constant of C_{44} of Sm_3Te_4 under magnetic fields parallel to the propagation direction [100] of the transverse ultrasonic wave. Solid line is a fit from Eq. (3) in the text with $T_0=14\,\mathrm{K}$ and $K=0.71\times10^{-4}$.

The elastic constants ρv^2 and the coupling parameters $K,\overline{P}\gamma^2$ in Sm_3Te_4 are listed in Table I. The parameters of the borosilicate glass and metallic glass $Pd_{70}Si_{16}Cu_6$ are also presented in Table I for comparison.[16,21–24] It should be noted that the constant $K=(0.44-1.4)\times10^{-4}$ and $\overline{P}\gamma^2=(0.14-0.52)\times10^8\,\mathrm{erg/cm^3}$ for the two-level system due to the $4f$-electron tunneling in Sm_3Te_4 has the same order of magnitude as the result in the amorphous glass compounds with the ionic tunneling state.

The internal magnetic field caused by the spin glass ordering may reduce the density of state $\overline{P}$ for the low-energy tunneling state in Sm_3Te_4. The elastic softening with $\ln T$ dependence, therefore, shows the upturn at the spin glass transition point. The cross marks, open circles, and open triangles in Fig. 9 are spin glass transition points determined by C_{11} in Fig. 6, $(C_{11}-C_{12})/2$ in Fig. 7, and C_{44} in Fig. 8, respectively. The magnetic phase diagram of Fig. 9 determined by the present ultrasonic experiment is consistent with the result obtained by the specific-heat measurement in fields.[11]

The saturation effect has been found in the low-temperature ultrasonic measurement for the two-level system of amorphous glass.[20] The electric pulse height for the generation of the input ultrasonic wave in the present low-temperature measurement was less than 0.1 V, which is estimated to be smaller than 0.1 μW.[25] This ensures that the

TABLE I. The parameters ρv^2, $\overline{P}\gamma^2$, and $K=\overline{P}\gamma^2/\rho v^2$ for the elastic softening due to the two-level system in Sm_3Te_4 at low temperatures by Eq. (3) in the text. Typical parameters of borosilicate glass, vitreous silica, and metallic glass of $Pd_{78}Si_{16}Cu_6$ are also listed for comparison (Refs. 16 and 21–24).

Sample	Mode	K	ρv^2 (erg/cm^3)	$\overline{P}\gamma^2$ (erg/cm^3)	γ (eV)
Sm_3Te_4	C_{11}	0.44×10^{-4}	8.90×10^{11}	0.39×10^{8}	
	$(C_{11}-C_{12})/2$	1.4×10^{-4}	3.73×10^{11}	0.52×10^{8}	
	C_{44}	0.71×10^{-4}	1.95×10^{11}	0.14×10^{8}	
Borosilicate glass	longitudinal	3.9×10^{-4}	9.0×10^{11}	2.3×10^{8}	0.3
	transverse	0.8×10^{-4}	1.4×10^{11}	1.1×10^{8}	
Vitreous silica	longitudinal	2.8×10^{-4}	7.4×10^{11}	2.1×10^{8}	0.4
$Pd_{78}Si_{16}Cu_6$	longitudinal	1.1×10^{-4}	14×10^{11}	1.5×10^{8}	0.4
	transverse	0.28×10^{-4}	3.4×10^{11}	0.1×10^{8}	

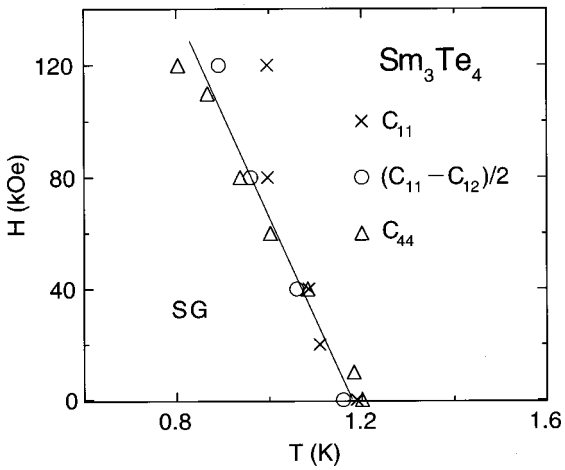

FIG. 9. Magnetic phase diagram for the spin glass transition of Sm_3Te_4 determined by the present ultrasonic measurements. Crosses and open triangles are obtained from C_{11}, C_{44} under the fields along [100]. Open circles are from $(C_{11}-C_{12})/2$ under field of [110].

present ultrasonic measurement with small input power is free from the saturation effect for the two-level system in Sm_3Te_4.

C. Analysis of the charge-fluctuation mode

It is naturally expected that the Coulomb interaction among trivalent and divalent ions favors the charge ordering in lowering temperature. We have previously reported the mechanism of the charge ordering in Yb_4As_3 with the anti-Th_3P_4 structure in the framework of the Landau phenomenological theory.[5] The present ultrasonic experiment, however, shows clearly the absence of the phase transition due to the charge ordering in Sm_3Te_4. In this section we analyze the charge-fluctuation modes and propose a mechanism for the charge glass state in Sm_3Te_4. Furthermore, we discuss the possibility of charge ordering in an isomorphous valence-fluctuation compound of Eu_3S_4 with the Th_3P_4-type structure.

In order to pick up charge-fluctuation modes in Sm_3Te_4, we apply the group-theoretical analysis in assuming the charge neutrality with the coexistence ratio $N(Sm^{2+}):N(Sm^{3+})=1:2$. This condition is satisfied in Sm_3Te_4 because of the absence of a carrier at low temperatures. Furthermore, we take only Sm ions into consideration for the analysis of the charge-fluctuation modes and we are not concerned with a mixing effect between $4f$ electrons of Sm and $5p$ electrons of Te.

We introduce the charge density $\rho_i\,(i=1,2,...,6)$ for the ith site of the Sm ion in Fig. 10 as a function of the position vector in units of the lattice parameter $a=9.5004$ Å of Sm_3Te_4:

$$\begin{aligned}
&\text{Sm1:}\quad \rho_1=\rho_1(\tfrac{3}{8},0,\tfrac{1}{4}),\\
&\text{Sm2:}\quad \rho_2=\rho_2(\tfrac{1}{8},0,\tfrac{3}{4}),\\
&\text{Sm3:}\quad \rho_3=\rho_3(\tfrac{3}{4},\tfrac{1}{8},0),\\
&\text{Sm4:}\quad \rho_4=\rho_4(\tfrac{1}{4},\tfrac{3}{8},0),
\end{aligned}\tag{4}$$

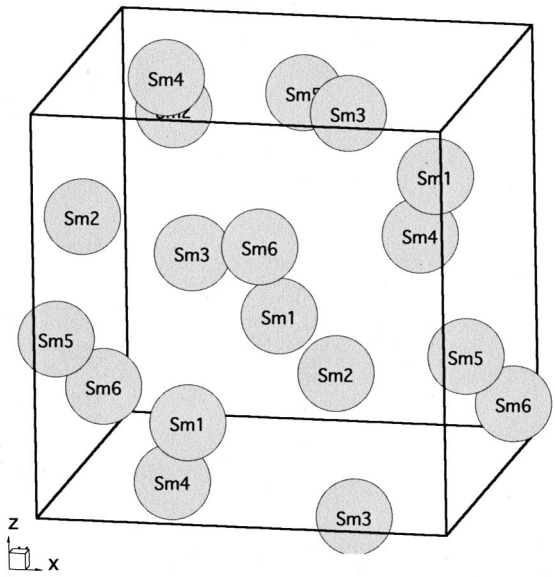

FIG. 10. Sm ions in the conventional unit cell of Sm_3Te_4 with the Th_3P_4-type structure belonging to space group T_d^6. Two crystallographically equivalent sites Smi $(i=1,2,\ldots,6)$ are included in the conventional unit cell because of the presence of body-centered symmetry.

$$\text{Sm5:}\quad \rho_5=\rho_5(0,\tfrac{1}{4},\tfrac{3}{8}),$$

$$\text{Sm6:}\quad \rho_6=\rho_6(0,\tfrac{3}{4},\tfrac{1}{8}),$$

Here the body-centered (bc) symmetry means that two crystallographically equivalent Sm sites in the conventional unit cell of Fig. 10 are related to the pure translation operator of $\{\mathbf{E}|\tfrac{1}{2}\,\tfrac{1}{2}\,\tfrac{1}{2}\}$ in the conventional unit cell.

One can derive the representation matrices with 6×6 elements by acting 24 symmetry operators of space group T_d^6 on ρ_i.[26] We obtain the characters by tracing of the representation matrices. The charge-fluctuation modes of Sm_3Te_4 with the Th_3P_4-type structure are decomposed into irreducible representations Γ_1 (1D), Γ_3 (2D), and Γ_4 (3D). Employing the projection operator, one obtains the bases for the irreducible representation in Table II.[27] The elastic strains characterized by Γ_1, Γ_3, and Γ_5 symmetries are also listed in Table II.

The charge density $\rho=\rho_0+\Delta\rho$ is introduced for the second-order phase transition in the Landau phenomenological theory. Here ρ_0 is the invariant term of the charge density in both phases above and below transition point T_c. The density of $\Delta\rho$ for a symmetry-breaking term is expanded by the product of the order parameter $Q_{\Gamma,\gamma}$ and the charge-fluctuation mode $\rho_{\Gamma,\gamma}$ as $\Delta\rho=\Sigma_{\Gamma,\gamma}Q_{\Gamma,\gamma}\rho_{\Gamma,\gamma}$. This term is $\Delta\rho=0$ above T_c and $\Delta\rho\neq0$ below T_c. In the case of Sm_3Te_4, the charge-fluctuation modes of either Γ_3 or Γ_4 with symmetry-breaking character can prove to be an active representation for the second-order transition. The constraint of integer charge unit e for the localized $4f$ electron in the ordered phase permits only $Q_{\Gamma3,u}$ for the $\rho_{\Gamma3,u}$ mode to be an order parameter. This point is discussed again later.

TABLE II. The charge-fluctuation mode and the elastic strain for the valence fluctuation compound Sm_3Te_4 of Th_3P_4-type structure with space group T_d^6. In the constraint of the localized character of the $4f$ electron in the present Sm_3Te_4 compound, the charge-fluctuation mode of $\rho_{\Gamma 3,u}=\rho_1+\rho_2+\rho_3+\rho_4-2\rho_5-2\rho_6$ in Fig. 11(a) permits the charge distribution with integer values of unit e.

Symmetry	Charge-fluctuation mode	Elastic strain
Γ_1	$\rho_{\Gamma 1}=\rho_1+\rho_2+\rho_3+\rho_4+\rho_5+\rho_6$	$\varepsilon_B=\varepsilon_{xx}+\varepsilon_{yy}+\varepsilon_{zz}$
Γ_3	$\rho_{\Gamma 3,u}=\rho_1+\rho_2+\rho_3+\rho_4-2\rho_5-2\rho_6$	$\varepsilon_u=(2\varepsilon_{zz}-\varepsilon_{xx}-\varepsilon_{yy})\sqrt{3}$
	$\rho_{\Gamma 3,v}=-\rho_1-\rho_2+\rho_3+\rho_4$	$\varepsilon_v=\varepsilon_{xx}-\varepsilon_{yy}$
Γ_4	$\rho_{\Gamma 4,x}=\rho_1-\rho_2$	
	$\rho_{\Gamma 4,y}=-\rho_3+\rho_4$	
	$\rho_{\Gamma 4,z}=\rho_5-\rho_6$	
Γ_5		ε_{yz}
		ε_{zx}
		ε_{xy}

It is important to note that the order parameter $Q_{\Gamma 3,u}$ for the charge-fluctuation mode $\rho_{\Gamma 3,u}$ and $Q_{\Gamma 3,v}$ for $\rho_{\Gamma 3,v}$ may couple to the tetragonal strain $\varepsilon_u=(2\varepsilon_{zz}-\varepsilon_{xx}-\varepsilon_{yy})/\sqrt{3}$ and the orthorhombic strain $\varepsilon_v=\varepsilon_{xx}-\varepsilon_{yy}$, respectively. This interaction term is written as

$$H_{\rm int}=g_{\Gamma 3}(Q_{\Gamma 3,u}\varepsilon_u+Q_{\Gamma 3,v}\varepsilon_v). \tag{5}$$

On the other hand, the charge-fluctuation mode with Γ_5 symmetry is absent in Sm_3Te_4. Therefore, the coupling of the charge-fluctuation mode to the elastic strain $\varepsilon_{yz},\varepsilon_{zx},\varepsilon_{xy}$ of the C_{44} mode is lacking.

The charge-fluctuation mode with Γ_1 symmetry $\rho_{\Gamma 1}=\rho_1+\rho_2+\rho_3+\rho_4+\rho_5+\rho_6$ represents uniform charge distribution all over the Sm sites with a mean valence of (8/3+). The Γ_1 charge-fluctuation mode may couple to the bulk strain $\varepsilon_B=\varepsilon_{xx}+\varepsilon_{yy}+\varepsilon_{zz}$, but this coupling does not play an important role in Sm_3Te_4 because of the absence of the softening in the bulk modulus $C_B=(C_{11}+2C_{12})/3$ in the experimental result of Fig. 2. This means that the coexistence ratio of Sm^{2+} and Sm^{3+} ions in Sm_3Te_4 remains constant even in lowering temperature. This result on Sm_3Te_4 is in contrast to the considerable softening of the bulk modulus C_B of the intermediate valence compound SmB_6, where the population of the Sm^{2+} ionic state increases in lowering temperature.[28]

The valence at each rare-earth site in the charge-ordered phase must be an integral multiple of the fundamental charge e, because of the localization of the $4f$ electron. Keeping this principle in mind, consider now the implications of the charge-fluctuation modes with symmetry-breaking character in Table II. The charge-fluctuation mode $\rho_{\Gamma 3,u}$ is the only mode which has the integer charge distribution in the unit of e. The Γ_3 mode of $\rho_{\Gamma 3,u}=\rho_1+\rho_2+\rho_3+\rho_4-2\rho_5-2\rho_6$ that couples to a tetragonal strain $\varepsilon_u=(2\varepsilon_{zz}-\varepsilon_{xx}-\varepsilon_{yy})/\sqrt{3}$ permits the location of the integer charge of 3+ at sites of Sm1, Sm2, Sm3, Sm4 and 2+ at sites of Sm5, Sm6 as shown in Fig. 11(a).

The mode of $\rho_{\Gamma 3,v}=-\rho_1-\rho_2+\rho_3+\rho_4$ in Fig. 11(b) may couple to an orthorhombic strain $\varepsilon_v=\varepsilon_{xx}-\varepsilon_{yy}$. The charge distribution of $\rho_{\Gamma 3,v}$ in Fig. 11(b), however, represents integer charge 3+ at sites of Sm3, Sm4, noninteger charge (7/3+) at sites of Sm1, Sm2, and (8/3+) at sites of Sm5, Sm6.

The analysis based on Eq. (5) leads to the possibility of a softening of $(C_{11}-C_{12})/2$ with Γ_3 symmetry in the compound. As shown in Fig. 2, however, the softening in $(C_{11}-C_{12})/2$ has not been found in the present experiment of Sm_3Te_4. This result means that the Γ_3 charge-fluctuation mode does not freeze even at low temperatures and suggests that the ground state of the charge-fluctuation modes in Sm_3Te_4 does not belong to the Γ_3 character.

In Fig. 11(c), we show the charge-fluctuation mode of $\rho_{\Gamma 4,x}=\rho_1-\rho_2$ as a representative of the Γ_4 triplet. The bilinear coupling of the charge-fluctuation mode $\rho_{\Gamma 4}$ to the elastic strain is absent, because the appropriate elastic strain with Γ_4 symmetry does not exist. The charge distribution of $\rho_{\Gamma 4,x}$ in Fig. 11(c) represents integer charge 3+ at the Sm1 site, while noninteger charge (7/3+) is located at the Sm2 site and (8/3+) at the Sm3, Sm4, Sm5, Sm6 sites.

The noninteger charge distribution is allowed only in a high-temperature side, where the charge fluctuation is available in the thermally activated process. On the other hand, only the integer charge location on Sm sites is realized in the ordered phase, because the localization of the $4f$ electron prohibits the noninteger charge distribution. In this context, the charge-fluctuation mode of $\rho_{\Gamma 3,u}$ in Fig. 11(a) is the only candidate for the charge-ordering state in the compounds with the Th_3P_4-type structure. In the present system of Sm_3Te_4, however, the charge ordering is absent and the charge glass state due to the random distribution of Sm^{2+} and Sm^{3+} ions is realized. A possibility of the charge ordering of $\rho_{\Gamma 3,u}$ in Eu_3S_4 is discussed in the following section.

The difference in the Madelung energy between the charge-fluctuation modes of Γ_1, Γ_3, and Γ_4 in Sm_3Te_4 is not clear at the present stage. When the Γ_4 mode is the ground state of the system, the freeze of the Γ_4 mode is expected at low temperatures. However, the ordered phase with the integer charge of the fundamental unit e at the Sm sites is impossible by the freeze of the Γ_4 mode. This is a probable scenario for the charge glass state of the random distribution of Sm^{2+} and Sm^{3+} ions in Sm_3Te_4 at low temperatures.

IV. CONCLUDING REMARKS

In this paper we present the elastic constant and the ultrasonic attenuation of the charge-fluctuation compound

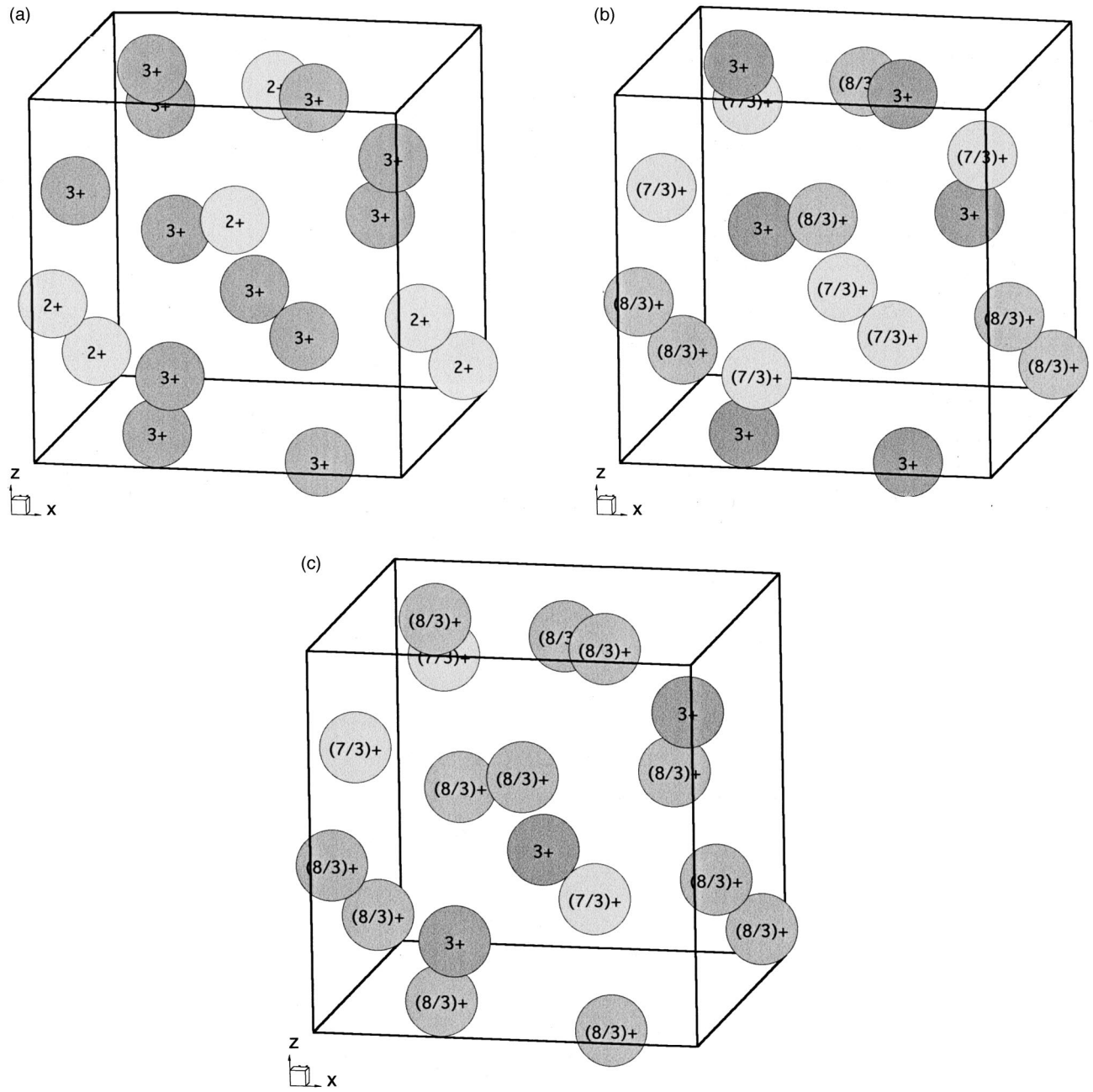

FIG. 11. (a) A charge-fluctuation mode of $\rho_{\Gamma 3,u}=\rho_1+\rho_2+\rho_3+\rho_4-2\rho_5-2\rho_6$ in Sm_3Te_4 with the Th_3P_4-type structure. In the charge-fluctuation mode of $\rho_{\Gamma 3,u}$, the trivalent Sm^{3+} ions occupy the sites of Sm1, Sm2, Sm3, Sm4 and the divalent Sm^{2+} ions locate the sites of Sm5, Sm6. The $\rho_{\Gamma 3,u}$ mode is a candidate for the charge ordering state in the valence-fluctuation compound with the Th_3P_4-type structure. (b) A charge-fluctuation mode of $\rho_{\Gamma 3,v}=-\rho_1-\rho_2+\rho_3+\rho_4$ in Sm_3Te_4 with Th_3P_4-type structure. In the $\rho_{\Gamma 3,v}$ mode, the integer charge 3+ is located at the Sm3, Sm4 site, while noninteger charge (7/3+) thermally populates at Sm1, Sm2 and (8/3+) at Sm5, Sm6 sites. (c) A charge-fluctuation mode of $\rho_{\Gamma 4,x}=\rho_1-\rho_2$ in Sm_3Te_4 with Th_3P_4-type structure. In the $\rho_{\Gamma 4,x}$ mode, the integer charge 3+ is located at the Sm1 site, while noninteger charge (7/3+) thermally populates at Sm2 and (8/3+) at Sm3, Sm4, Sm5, Sm6 sites.

Sm_3Te_4. It was found that Sm_3Te_4 shows the ultrasonic dispersion due to the charge fluctuation of $4f$ electrons among Sm^{2+} and Sm^{3+} ions. Even though the charge-fluctuation time $2\pi\tau$ of Sm_3Te_4 becomes infinite in lowering temperature, the phase transition associated with the charge ordering has not been found. This means that the charge fluctuation in Sm_3Te_4 freezes to be the charge glass state with the random distribution of Sm^{2+} and Sm^{3+} ions.

At low temperatures we observed the characteristic softening of the elastic constants C_{11}, $(C_{11}-C_{12})/2$, and C_{44} proportional to $\ln T$. This result strongly suggests that the two-level system of the $4f$ electrons tunneling among Sm^{2+} and Sm^{3+} ions exists although the lattice of Sm_3Te_4 has a perfect periodicity. The $\ln T$ dependence of the elastic constant, the large specific-heat coefficient of C/T, and the spin glass phase in Sm_3Te_4 are consistent with the scenario of the two-level system of the $4f$-electron tunneling in the random potential of Sm^{2+} and Sm^{3+} ions.

We made the group-theoretical analysis of the charge fluctuation in the compound with the Th_3P_4 structure under

the condition of charge neutrality. The charge-fluctuation modes are decomposed into irreducible representations of Γ_1, Γ_3, and Γ_4. When the charge-fluctuation mode with Γ_4 symmetry is the ground state, the ordered phase associated with integer charge of unit e is impossible. In the present case of Sm_3Te_4, therefore, we may suggest that the freezing of the Γ_4 mode gives rise to the charge glass state because of the charge frustration effect. The constraint of the charge unit e for the localized $4f$ electrons at the Sm site prevents the long-range ordering of the Γ_4 mode.

The charge-fluctuation mode $\rho_{\Gamma 3,u}=\rho_1+\rho_2+\rho_3+\rho_4-2\rho_5-2\rho_6$ is the only candidate for the order parameter of the charge ordering with the integer charge of unit e in the Th_3P_4-type compound. The freeze of the charge-fluctuation mode $\rho_{\Gamma 3,u}$ may lead a structural phase transition from cubic to tetragonal. It is quite interesting that the isomorphous compound Eu_3S_4 with the Th_3P_4-type structure exhibits the charge ordering due to Eu^{2+} and Eu^{3+} ions at $T_c=186$ K.[29] The thermal expansion on Eu_3S_4 measurement suggests the tetragonal distortion at T_c. The neutron experiment of Eu_3S_4, however, pointed out the trigonal distortion along the [111] direction at T_c.[30] As was presented already, the ordering of the charge-fluctuation mode $\rho_{\Gamma 3,u}$ in Fig. 11(a) leads naturally to the lattice distortion from cubic to tetragonal phase with a spontaneous strain $\varepsilon_u=(2\varepsilon_{zz}-\varepsilon_{xx}-\varepsilon_{yy})/\sqrt{3}$ at T_c. Furthermore, the elastic softening of $(C_{11}-C_{12})/2$ is expected around T_c. In order to obtain a scenario for the charge ordering in Eu_3S_4, x-ray and ultrasonic investigations on the compounds are desired.

ACKNOWLEDGMENTS

The authors are grateful to Professor M. Goda and Professor T. Nakayama for valuable discussions on the two-level system. This work was partly supported by the Grant-in-Aid for Scientific Research from the Ministry of Education, Science and Culture of Japan.

[1] C. M. Varma, Rev. Mod. Phys. **48**, 219 (1976).
[2] F. L. Carter, J. Solid State Chem. **5**, 300 (1972).
[3] A. Ochiai, Master thesis, Tohoku University, 1979.
[4] J. M. D. Coey, B. Cornut, F. Holtzberg, and S. von Molnar, J. Appl. Phys. **50**, 1923 (1979).
[5] T. Goto, Y. Nemoto, A. Ochiai, and T. Suzuki, Phys. Rev. B **59**, 269 (1999).
[6] B. Batlogg, E. Kaldis, A. Schlegel, G. von Schulthess, and P. Wachter, Solid State Commun. **19**, 673 (1976).
[7] H. Goto, K. Baba, T. Goto, S. Nakamura, A. Tamaki, A. Ochiai, T. Suzuki, and T. Kasuya, J. Phys. Soc. Jpn. **62**, 1365 (1993).
[8] A. Tamaki, T. Goto, S. Kunii, T. Suzuki, T. Fujimura, and T. Kasuya, J. Phys. C **18**, 5849 (1985).
[9] S. von Molnar, F. Holtzberg, A. Benoit, A. Briggs, J. Flouquet, and J. L. Tholence, *Valence Instabilities* (North-Holland, Amsterdam, 1982), p. 597.
[10] K. Fraas, U. Ahlheim, P. H. P. Reinders, C. Schank, R. Caspary, F. Steglich, A. Ochiai, T. Suzuki, and T. Kasuya, J. Magn. Magn. Mater. **108**, 220 (1992).
[11] H. Aoki and A. Ochiai (private communication).
[12] T. Tayama, K. Tenya, H. Amitsuka, T. Sakakibara, A. Ochiai, and T. Suzuki, J. Phys. Soc. Jpn. **65**, 3467 (1996).
[13] P. A. Alekseev, P. Fabi, J.-M. Mignot, E. V. Nefeodova, A. Ochiai, and S. A. Riazantsev, Physica B **234-236**, 883 (1997).
[14] P. W. Anderson, B. I. Halperin, and C. M. Varma, Philos. Mag. **25**, 1 (1972).
[15] J. Jäckle, Z. Phys. **257**, 212 (1972).
[16] S. Hunklinger and W. Arnold, *Physical Acoustics* (Academic, New York, 1976), Vol. XII, p. 155.
[17] T. Nakayama, J. Phys. Soc. Jpn. **68**, 3540 (1999).
[18] T. Nakayama and K. Yakubo, *Proceedings of the 5th International Conference on Phonon Scattering in Condensed Matter*, edited by A. C. Anderson and J. P. Wolfe, Springer Series in Solid State Science Vol. 68 (Springer, Berlin, 1986), p. 94.
[19] R. C. Zeller and R. O. Pohl, Phys. Rev. B **4**, 2029 (1971).
[20] *Amorphous Solids: Low-Temperature Properties*, edited by W. A. Phillips (Springer, Berlin, 1981).
[21] T. L. Smith, P. J. Anthony, and A. C. Anderson, Phys. Rev. B **17**, 4997 (1978).
[22] P. Esquinazi, R. König, and F. Pobell, Z. Phys. B: Condens. Matter **87**, 305 (1992).
[23] A. K. Raychaudhuri and S. Hunklinger, Z. Phys. B: Condens. Matter **57**, 113 (1984).
[24] U. Buchenau, Yu. M. Galperin, V. L. Gurevich, and H. R. Schober, Phys. Rev. B **43**, 5039 (1991).
[25] T. Goto, S. Sakatsume, A. Sawada, H. Matsui, R. Settai, S. Nakamura, Y. Ohtani, H. Goto, Y. Ohe, A. Tamaki, Y. Fuda, K. Abe, Y. Yamato, and T. Fujimura, Cryogenics **32**, 902 (1992).
[26] *International Tables for Crystallography Volume A*, edited by Theo Hahn (Kluwer Academic Publishers, Dordrecht, 1989).
[27] T. Inui, Y. Tanabe, and Y. Onodera, *Group Theory and Its Applications in Physics* (Springer, Berlin, 1990).
[28] S. Nakamura, T. Goto, M. Kasaya, and S. Kunii, J. Phys. Soc. Jpn. **60**, 4311 (1991).
[29] R. Pott, G. Güntherodt, W. Wichelhaus, M. Ohl, and H. Bach, Phys. Rev. B **27**, 359 (1983).
[30] W. Wickelhaus, A. Simon, K. W. H. Stevens, P. J. Brown, and K. R. A. Ziebeck, Philos. Mag. B **46**, 115 (1982).